

Thermal ionization of excitons in V-shaped quantum wires

Original

Thermal ionization of excitons in V-shaped quantum wires / Rinaldi, R.; Giugno, P. V.; Cingolani, R.; Rossi, Fausto; Molinari, E.; Marti, U.; Reinhart, F. K.. - In: PHYSICAL REVIEW. B, CONDENSED MATTER. - ISSN 0163-1829. - 53:20(1996), pp. 13710-13714. [10.1103/PhysRevB.53.13710]

Availability:

This version is available at: 11583/2498579 since:

Publisher:

APS

Published

DOI:10.1103/PhysRevB.53.13710

Terms of use:

This article is made available under terms and conditions as specified in the corresponding bibliographic description in the repository

Publisher copyright

(Article begins on next page)

Thermal ionization of excitons in V-shaped quantum wires

R. Rinaldi, P. V. Giugno, and R. Cingolani

Istituto Nazionale per la Fisica della Materia (INFM) and Dipartimento Scienza dei Materiali, Università di Lecce, I-73100 Lecce, Italy

F. Rossi

Fachbereich Physik, Philipps-Universität Marburg, D-35032 Marburg, Germany

E. Molinari

Istituto Nazionale per la Fisica della Materia (INFM) and Dipartimento di Fisica, Università di Modena, I-41100 Modena, Italy

U. Marti and F. K. Reinhart

Ecole Polytechnique Fédérale de Lausanne, PHB Ecublens, CH-1015 Lausanne, Switzerland

(Received 24 October 1995; revised manuscript received 19 December 1995)

The exciton-to-free-carrier transition in GaAs and $\text{In}_x\text{Ga}_{1-x}\text{As}$ V-shaped quantum wires is revealed by means of temperature-dependent magnetoluminescence experiments. The experimental results are in excellent agreement with the diamagnetic shift obtained from a solution of the full two-dimensional Schrödinger equation for electrons and holes including magnetic-field and excitonic effects. In the GaAs wires, the exciton-to-free-carrier transition is found to occur at temperature consistent with the exciton binding energies. In the $\text{In}_x\text{Ga}_{1-x}\text{As}$ wires the diamagnetic shift of the luminescence is found to be free-carrier-like, independent of temperature, due to the weakening of the exciton binding energy induced by the internal piezoelectric field.

I. INTRODUCTION

Technological progress in the fabrication of high-quality V-groove quantum-wire structures^{1,2} has allowed only recently a detailed investigation of quasi-one-dimensional excitons. The exciton binding energy of GaAs quantum wires of 20-nm lateral width has been determined experimentally by two-photon absorption and magnetoluminescence studies,^{3,4} and compared with excitonic models based on variational approaches^{4,5} or on the more advanced solution of the semiconductor Bloch equations.⁶

In this paper we study the thermodynamical properties of quantum wire excitons by means of temperature-dependent magnetoluminescence experiments. The transition from excitonic to free-carrier recombination is directly monitored through the change of the diamagnetic shift of the luminescence occurring above the ionization temperature of the exciton in both GaAs and $\text{In}_x\text{Ga}_{1-x}\text{As}$ quantum wires. The quantitative analysis of the experimental data is based on a solution of the full two-dimensional Schrödinger equation both for the one-dimensional magnetoexciton and for the free-carrier case (i.e., neglecting electron-hole correlation). We find that when excitons are thermally dissociated a clear change of diamagnetic shift occurs in GaAs quantum wires. Conversely, the transition does not appear in $\text{In}_x\text{Ga}_{1-x}\text{As}$, where the diamagnetic shift exhibits a clear free-carrier behavior at all temperatures. This is ascribed to the weakened exciton binding energy caused by the strong internal piezoelectric field existing in the strained $\text{In}_x\text{Ga}_{1-x}\text{As}/\text{GaAs}$ quantum wires.

II. EXPERIMENT

The GaAs substrates were patterned in the form of V-shaped grooves by holographic lithography and wet

chemical etching. The wires originated from the bending of thin quantum wells deposited by molecular beam epitaxy onto the grooves. The grown heterostructures consist of 18 ML of GaAs or $\text{In}_x\text{Ga}_{1-x}\text{As}$ ($x=0.12$) embedded between two $(\text{GaAs})_8/(\text{AlAs})_4$ superlattices (values calibrated for the planar growth). Due to the preferential growth at the bottom of the groove, the thickness of the deposited quantum well ranges from about 10 nm at the bottom of the groove to 2 nm on the sidewalls. The lateral shrinkage of the deposited well provides the additional confining potential originating the one-dimensional effects.^{1,2} The samples were characterized by transmission electron microscopy, in order to obtain the quantum-wire cross section from which the lateral potential was determined. Photoluminescence (PL) and photoluminescence-excitation (PLE) measurements were performed by using an infrared extended Ti:sapphire laser and a double 0.85-m monochromator equipped with cooled photon counting. The magnetoluminescence measurements were performed in a superconducting magnet providing fields up to 10 T in the temperature range 2.2 K – 300 K. The spectral resolution in all measurements was always better than 2 Å.

III. THEORY

To interpret the magnetoluminescence data, we need a reliable description of both single-particle and excitonic properties in the V-grooved structures, as well as their modification induced by the applied magnetic field.

Because of the V-shaped profile of the confining potential, no analytical solutions are available for the electronic structure, even in the simplest envelope-function approximation. Therefore, we first compute numerically the electron and hole wave functions for the various quantum-wire subbands and the corresponding energy levels, using as an input

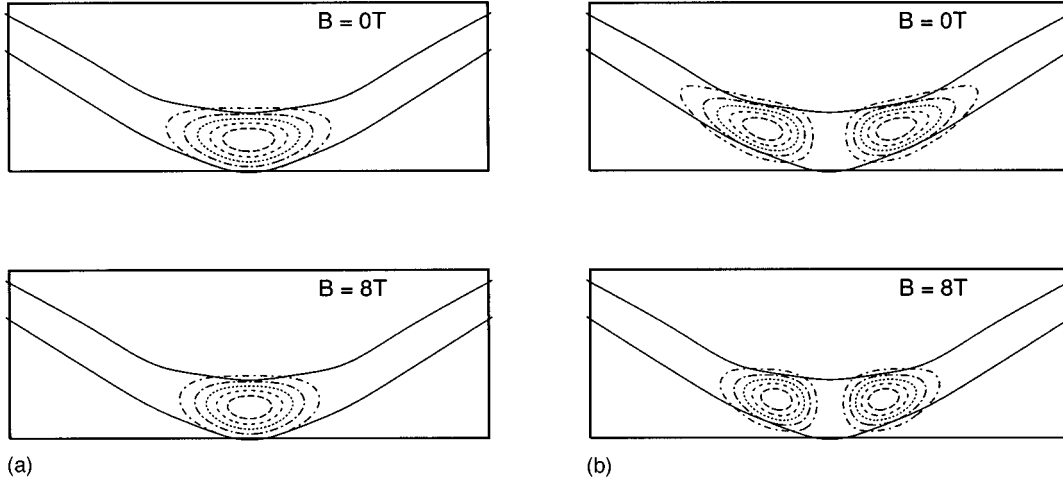


FIG. 1. (a) Charge-density contour plot of the first conduction subband of the wire for $B=0$ and 8 T. (b) Charge-density contour plot associated to the second conduction subband of the wire for $B=0$ and 8 T. The solid line represents schematically the wire cross section. The region depicted here is only a small portion of the groove: the lengths of the horizontal (y) and vertical (z) axes are 70 and 25 nm, respectively.

the shape of the confining potential as determined by transmission electron microscopy. Starting from this single-particle representation, we obtain the linear-absorption spectrum by numerical solution of the semiconductor Bloch equations for our multisubband wire structure. This provides a self-consistent description of both single-particle and excitonic properties of the system.

A. Single-particle analysis

Let us first consider noninteracting electrons (e) and holes (h), subject to a confining potential V_c^e or V_c^h whose height is dictated by the conduction–valence-band discontinuities. In the energy region of interest, we can adopt the usual effective-mass and envelope-function approximations.

By denoting with z the free wire direction, the carrier wave function can be factorized in terms of a plane wave along the free direction (with wave vector component k_z) times an envelope function $\phi_v^{e/h}(x,y)$ solution of the two-dimensional (2D) Schrödinger equation

$$\left[-\frac{\hbar^2}{2m^{e/h}} \left(\frac{\partial^2}{\partial^2 x} + \frac{\partial^2}{\partial^2 y} \right) + V_c^{e/h}(x,y) \right] \phi_v^{e/h}(x,y) = \mathcal{E}_v^{e/h} \phi_v^{e/h}(x,y). \quad (1)$$

Here $m^{e/h}$ are the bulk effective masses of electrons and holes. The band structure for a carrier in the wire,

$$\mathcal{E}_{k_z v}^{e/h} = \mathcal{E}_v^{e/h} + \frac{\hbar^2 k_z^2}{2m^{e/h}}, \quad (2)$$

and the corresponding wave functions are then obtained numerically by direct solution of the single-particle Eq. (1) in terms of a plane-wave representation with periodic boundary conditions.

This approach is easily extended to account for an applied homogeneous magnetic field $\mathbf{B} = (B_x, B_y, B_z)$, which can be described in terms of the following vector potential:

$$\mathbf{A} = (0, B_z x, B_x y - B_y x). \quad (3)$$

This particular choice of the vector potential, which results in a function of x and y only, still allows the factorization of the wave function previously discussed. The 2D Schrödinger equation then maintains the same structure, but it includes in the potential an additional term due to the applied magnetic field:⁷

$$\mathcal{H}_{k_z}^{e/h}(x,y) = \frac{i\hbar e B_z x}{m^{e/h}} \frac{\partial}{\partial y} - \frac{\hbar k_z e}{m^{e/h}} (B_x y - B_y x) + \frac{e^2}{2m^{e/h}} [(B_z x)^2 + (B_x y - B_y x)^2]. \quad (4)$$

As in the previous case, the 2D Schrödinger equation can be solved by direct diagonalization in the same plane-wave basis. Note, however that, contrary to the case $B=0$, the resulting eigenvalue and eigenvector spectra are now a function of the wave vector k_z .

It is important to comment on two approximations adopted in the present model. First, valence-band mixing (VBM) is not included. We believe that this approximation is not critical for the purpose of this paper. Indeed, while it is known that VBM introduces significant corrections on absolute values of exciton binding energies⁸ and affects selection rules because of the modified wave functions,^{9,10} recent calculations clearly indicate that it should not be important for the lowest states considered here.¹¹ Second, we have neglected the Zeeman term in Eq. (4);⁷ as shown in Ref. 10, this is expected to affect the present results only very marginally.

The output of our single-particle calculations for the wave functions are exemplified in Fig. 1, where we plot the charge-density contour plots of the $n=1$ and electron states confined in the GaAs quantum wires. The wave functions are squeezed by the transverse magnetic field with a consequent increase of the localization energy. The diamagnetic shift of the electron eigenstates is found to be quadratic in the field; the strength of the total shift increases with the subband quantum number, reflecting the increased delocalization of the carrier wave functions. The resulting shift in the single-

particle transitions for $n=1$ will be compared with experimental data in Sec. IV (see Fig. 3 below).

Note that the theoretical evaluation of quantized states in $\text{In}_x\text{Ga}_{1-x}\text{As}$ V-shaped wires is more complicated due to the presence of a nontetragonal strain deformation at the $\text{In}_x\text{Ga}_{1-x}\text{As}$ -GaAs interfaces along the $\{111\}$ facets.^{12–15} The nondiagonal terms of the strain tensor originate a piezoelectric field at the heterointerfaces. Following Ref. 12, the internal piezoelectric potential is obtained by a triple integration of the charge density ($\rho = \text{div}\mathbf{P}$). The polarization vector components are given by $P_i = e_{14}\epsilon_{jk}$ ($i \neq j \neq k$), where e_{14} is the piezoelectric modulus and ϵ_{jk} are the nondiagonal strain tensor elements. The local value of the strain field is calculated based on the elasticity theory for a coherently strained semiconductor heterostructure oriented along an arbitrary $n(xyz)$ direction, according to Ref. 14. Details on these calculations will be reported elsewhere.¹⁵ The obtained piezoelectric field for the $\text{In}_{0.12}\text{Ga}_{0.88}\text{As}$ wires ranges between zero at the bottom of the groove and 1.5×10^4 V/cm at the top of the quantum-wire sidewalls. The internal field is perpendicular to the sidewalls and affects the electronic states in different ways: namely, it breaks the symmetry of the valence states,¹² slightly changes the potential offset (this results in a reduction of the quantization energies of the order of 10% in our quantum wires,^{12,15}), and reduces the exciton binding energy by about 40%.¹⁶ The potential modified by piezoelectric effects has been used in all our calculations for $\text{In}_x\text{Ga}_{1-x}\text{As}$ -based wires.

B. Excitonic effects

To study the optical properties of our quantum wires, we now consider the effects of electron-hole correlation. Our

approach is based on a generalization^{6,17} of the well-known semiconductor Bloch equations^{18–20} (SBE's) to a multisubband wire structure. Our SBE's provide a kinetic description of the system in terms of the various distribution functions of electrons and holes $f_{k_z\nu}^{e/h}$ as well as the corresponding diagonal ($\nu^e = \nu^h = \nu$) interband polarizations $p_{k_z\nu}$.

Here we focus on the linear response of the system close to the band gap, i.e., the excitonic regime. Therefore, all incoherent phenomena (e.g., carrier-phonon and carrier-carrier scattering) can be neglected. Moreover, we focus on the linear-response regime in which the solution of the set of SBE's simply reduces to the solution of the following equation for the interband polarization:

$$i\hbar \frac{d}{dt} p_{k_z\nu} = (\mathcal{E}_{k_z\nu}^e + \mathcal{E}_{-k_z\nu}^h) p_{k_z\nu} + [M_{k_z\nu} A_0(t) e^{-i\omega_L t} + \Delta_{k_z\nu}]. \quad (5)$$

Here, $A_0(t)$ is the envelope of the vector potential of the laser field with angular frequency ω_L . $\mathcal{E}_{k_z\nu}^{e,h}$ are the free-carrier energies, while $M_{k_z\nu}$ is the dipole matrix element. $\Delta_{k_z\nu}$ is the internal field,¹⁸ which in the Hartree-Fock approximation is given by¹⁸

$$\Delta_{k_z\nu} = - \sum_{k_z'\nu'} V_{k_z\nu, k_z'\nu'; k_z\nu, k_z'\nu'}^c p_{k_z'\nu'}, \quad (6)$$

where

$$V_{k_z^1\nu^1, k_z^2\nu^2; k_z^3\nu^3, k_z^4\nu^4}^c = \int d\mathbf{r} \int d\mathbf{r}' \phi_{k_z^1\nu^1}^{e*}(\mathbf{r}) \phi_{k_z^2\nu^2}^{h*}(\mathbf{r}') V^c(\mathbf{r} - \mathbf{r}') \phi_{k_z^3\nu^3}^h(\mathbf{r}') \phi_{k_z^4\nu^4}^e(\mathbf{r}) \quad (7)$$

are the electron-hole matrix elements of the Coulomb potential V^c .

The stationary solutions of this equation can then be obtained by direct diagonalization in the basis of the single-particle states of the previous paragraph. They are the polarization eigenvalues and eigenvectors, which fully determine the absorption spectrum as well as the exciton wave function. The resulting excitonic recombination peaks show a parabolic shift quadratic in the field (solid lines in Fig. 3 below), as in the case of single-particle transitions. Such shift is, however, of smaller strength with respect to the shift of the subband edge (dashed lines in the same figure).

IV. EXPERIMENTAL RESULTS AND DISCUSSION

The samples chosen for this study exhibit well-resolved one-dimensional features in the optical spectra and excellent optical quality. In Fig. 2 we show the photoluminescence and photoluminescence-excitation spectra of a representative

$\text{In}_{0.12}\text{Ga}_{0.88}\text{As}$ quantum wire of lateral width 16 nm. The PL lines show a clear band-filling spectrum due to recombination of the $n=2$ and 3 excitons. The PLE spectrum exhibits three resonances with the same energy separation of the PL spectrum. The Stokes shift amounts to about 6 meV, in agreement with the broadening of the PL and PLE structures that can be attributed to the very weak In diffusion occurring in the ternary alloy wire.²¹ These spectra clearly evidence the one-dimensional character of the investigated quantum wire structures.

In Fig. 3 we display the temperature-dependent diamagnetic shift of the GaAs and $\text{In}_x\text{Ga}_{1-x}\text{As}$ wires, and compare it with the theoretical predictions for single-particle and excitonic transitions obtained as described in Sec. III. The ground-state exciton binding energy of the investigated GaAs wires is about 12 meV.^{4,6} Therefore, for temperatures of the order of 150 K excitons are expected to be ionized and the emission process must involve free carriers. This is clearly seen in Fig. 3(a). At 4 K the diamagnetic shift is

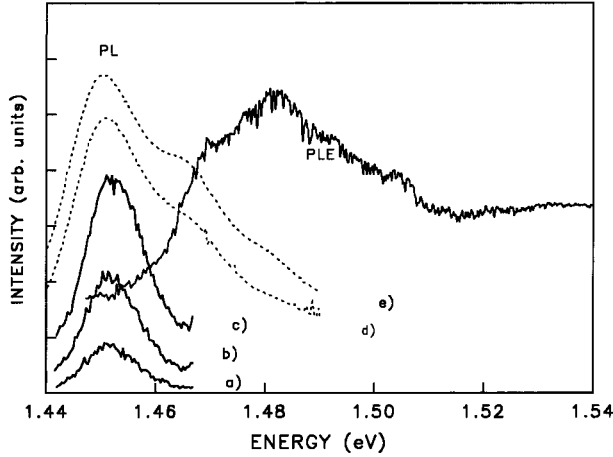


FIG. 2. Photoluminescence excitation and photoluminescence spectra of a 16-nm $\text{In}_{0.12}\text{Ga}_{0.88}\text{As}/\text{GaAs}$ quantum wire with superlattice barriers $[(\text{GaAs})_8/(\text{AlAs})_4]$. The photoluminescence spectra were obtained under resonant excitation at 842 nm (continuous lines) and off-resonant excitation at 514 nm (dashed lines). The power densities are (a) $I = 750 \text{ W cm}^{-2}$, (b) $I = 2.1 \text{ W cm}^{-2}$, (c) $I = 6.2 \text{ W cm}^{-2}$, (d) $I = 7.5 \text{ W cm}^{-2}$, (e) $I = 15 \text{ W cm}^{-2}$.

rather small, and it is well reproduced by the excitonic diamagnetic shift evaluated theoretically [solid line in Fig. 3(a)]. The shift remains excitonic at low temperatures (40 K). Around 120 K we observe some change in the magnetic field dependence of the diamagnetic shift, suggesting that excitons begin to dissociate and an exciton-free-carrier gas forms in the structure. Above 120 K the shift of the magnetoluminescence increases considerably with increasing field, and follows the expected free-carrier shift [dashed lines in Fig. 3(a)]. This indicates that the transition from excitonic to free-carrier recombination has occurred in the investigated temperature range.

In the case of $\text{In}_x\text{Ga}_{1-x}\text{As}$ wires [Fig. 3(b)] the situation is somewhat more complicated. The internal piezoelectric field reduces the exciton binding energy and the transition from excitonic to free-carrier recombination should occur at lower temperature than in GaAs. Actually, we do not observe any transition in the temperature-dependent magnetoluminescence spectra, as shown in Fig. 3(b). In particular, the diamagnetic shift is found to follow the free-carrier shift in the whole investigated temperature range.²² These results suggest that a theoretical modeling of the diamagnetic shift must take into account that the magnetic interaction affects excitons or free carriers depending on the actual extension of the exciton wave function. In particular, when the magnetic length $l = \sqrt{\hbar/eB}$ is smaller than the extent of the exciton wave function (i.e., the Bohr radius a_0), the magnetic interaction involves directly the individual electron and hole wave functions, resulting in a free-carrier shift.²³ On the other hand, an excitonic shift should be observed for $l > a_0$. It is difficult to evaluate the occurrence of this condition from our experiments. Below 4 T the calculated excitonic and free-carrier shifts are almost indistinguishable, and the comparison with the experimental data does not clarify the recombination mechanism. Above this field the experi-

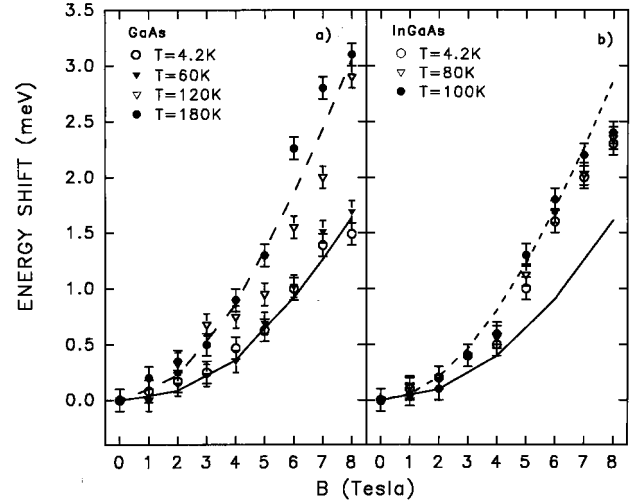


FIG. 3. (a) Diamagnetic shift of the $n = 1$ luminescence band of the GaAs wires at different temperatures (symbols). Lines represent theoretically evaluated shifts for excitons (solid lines) and for free carriers (dashed lines). (b) Same as in (a) for the $\text{In}_x\text{Ga}_{1-x}\text{As}$ wires.

mental data and the theory indicate rather clearly the occurrence of free-carrier recombination. This puts the upper limit of 4 T for the occurrence of a diamagnetic shift of excitonic origin in these $\text{In}_x\text{Ga}_{1-x}\text{As}$ wires. Such a value roughly corresponds to an exciton binding energy of the order of 5 meV. This is in turn consistent with a reduction of the exciton binding energy due to the piezoelectric field of about 40% with respect to the value expected for the 16-nm $\text{In}_x\text{Ga}_{1-x}\text{As}$ wire investigated here [about 9.5 meV (Ref. 24)], analogous to the quantum-well case.¹⁶

In conclusion, the thermal ionization of quasi-one-dimensional excitons has been revealed by means of magnetoluminescence experiments. For GaAs quantum wires a clear excitonic diamagnetism is observed in the luminescence spectra as long as the crystal temperature is smaller than the thermal activation energy of the exciton (i.e., the exciton binding energy). At higher temperatures free-carrier recombination becomes dominant, showing an enhancement of the diamagnetic shift. In the $\text{In}_x\text{Ga}_{1-x}\text{As}$ quantum wires a free-carrier diamagnetic shift is observed at all temperatures, which is interpreted as a consequence of the weakened exciton binding energy caused by the internal piezoelectric field existing in the strained wires.¹² In both cases the experimental results are in excellent agreement with the calculated shift of the magnetoexcitons and band-gap edge, obtained from a numerical solution of the two-dimensional Schrödinger equation describing our V-like quantum-wire structure. Diamagnetism is thus demonstrated to be a very sensitive probe for wave-function confinement in quantum wires.

We gratefully acknowledge G. Goldoni for useful discussions and D. Cannoletta, M. Corrado, P.C. Silva, and Y. Magnenat for their help in the experiments and in the sample preparation. Funding from the European Community (Nanopt Esprit project) and from the National Swiss Foundation (Swiss Priority Program in Optics) are gratefully acknowledged.

- ¹E. Kapon, in *Semiconductors and Semimetals* (Academic, New York, 1994), Chap. 4, p. 259.
- ²R. Cingolani and R. Rinaldi, *Nuovo Cimento* **6**, 1 (1993).
- ³R. Rinaldi *et al.*, M. Ferrara, R. Cingolani, U. Marti, D. Martin, F. Morier-Gemoud, P. Ruterana, and F.K. Reinhart, *Phys. Rev. B* **50**, 11 795 (1994).
- ⁴R. Rinaldi *et al.*, *Phys. Rev. Lett.* **73**, 2899 (1994).
- ⁵P. Christol, P. Lefebvre, and H. Mathieu, *J. Appl. Phys.* **74**, 5626 (1993).
- ⁶F. Rossi, E. Molinari, R. Rinaldi, and R. Cingolani, *Solid State Electron.* (to be published); also in *Proceedings of the International Conference on Modulated Semiconducting Structures* (Madrid, 1995), Vol. 1, p. 415.
- ⁷L. Landau and E. Lifchitz, *Mécanique Quantique. Théorie non relativiste*, 2nd ed. (Mir, Moscow, 1967), Chap. XV.
- ⁸See, e.g., L.C. Andreani, A. Pasquarello, and F. Bassani, *Phys. Rev. B* **36**, 5887 (1987).
- ⁹U. Bockelmann and G. Bastard, *Phys. Rev. B* **45**, 1688 (1992).
- ¹⁰G. Goldoni and A. Fasolino, *Phys. Rev. B* **52**, 14 118 (1995).
- ¹¹The quantum wires with rectangular section that are studied in Ref. 10 ($100 \times 300 \text{ \AA}$) are comparable in size with our structures. There, the lowest hole state in the wire is found to have 98% heavy-hole (HH) character in the absence of magnetic field, and 89% heavy-hole (HH) character at $B=10 \text{ T}$. This suggests that even for the maximum field used here ($B=10 \text{ T}$) the lowest hole state in our wires should be essentially HH-like, the light-hole contribution not exceeding 10%. The neglect of VBM would of course be more questionable in studies of higher transitions or polarization dependent features (Ref. 9).
- ¹²M. Grundmann, O. Stier, and D. Bimberg, *Phys. Rev. B* **50**, 14 187 (1994).
- ¹³L. DeCaro and L. Tapfer, *Phys. Rev. B* **51**, 4381 (1995).
- ¹⁴L. DeCaro and L. Tapfer, *Phys. Rev. B* **48**, 2298 (1993).
- ¹⁵R. Rinaldi, R. Cingolani, L. DeCaro, M. Lomascio, M. DiDio, L. Tapfer, U. Marti, and F.K. Reinhart, *J. Opt. Soc. Am. B* (to be published).
- ¹⁶M. Livingstone, I. Galbraith, and B.S. Wherrett, *Appl. Phys. Lett.* **65**, 2771 (1994).
- ¹⁷F. Rossi and E. Molinari, *Phys. Rev. Lett.* (to be published).
- ¹⁸H. Haug and S.W. Koch, *Quantum Theory of the Optical and Electronic Properties of Semiconductors*, 3rd ed. (World Scientific, Singapore, 1994).
- ¹⁹T. Kuhn and F. Rossi, *Phys. Rev. Lett.* **69**, 977 (1992); *Phys. Rev. B* **46**, 7496 (1992).
- ²⁰E. Binder, T. Kuhn, and G. Mahler, *Phys. Rev. B* **50**, 18 319 (1994).
- ²¹M. Pfister, M.B. Johnson, S.F. Alvarado, H.W.M. Salemink, U. Marti, D. Martin, F. Morier-Genoud, and F.K. Reinhart, *Appl. Phys. Lett.* **67**, 1459 (1995).
- ²²The total free-carrier shift in $\text{In}_x\text{Ga}_{1-x}\text{As}$ wires is smaller than in GaAs because of the difference in the heavy-hole effective masses. In fact, the values used for the $\text{In}_x\text{Ga}_{1-x}\text{As}$ and GaAs electron effective mass are $0.0614m_0$ and $0.0667m_0$, respectively, while for the heavy-hole mass they amount to $0.348m_0$ and $0.34m_0$, respectively. In the calculations the following V_e and V_h values have been used: $V_e=200 \text{ meV}$ and $V_h=133.6 \text{ meV}$ for GaAs, and $V_e=257 \text{ meV}$ and $V_h=208 \text{ meV}$ for $\text{In}_x\text{Ga}_{1-x}\text{As}$.
- ²³P.V. Giugno, A.L. Convertino, R. Rinaldi, R. Cingolani, J. Masies, and M. Leroux, *Phys. Rev. B* **52**, R1159 (1995).
- ²⁴This value is obtained starting from the exciton binding energy of the planar quantum well from which the wire is formed, and assuming the 25% enhancement measured in GaAs wires of similar size, as in Ref. 4.